

The core dominance parameter of extragalactic radio sources[★]

J. H. Fan and J. S. Zhang

Center for Astrophysics, Guangzhou University, Guangzhou 510400, PR China
e-mail: fjh@gzhu.edu.cn

Received 20 January 2003 / Accepted 12 June 2003

Abstract. In this paper, based on a paper by Liu and Zhang (2002), we have chosen a sample of 542 extragalactic sources (27 BL Lac objects, 300 galaxies (radio galaxies and Seyfert galaxies), and 215 quasars), for which we have calculated the core-dominance parameters and investigated the relation between core-dominance parameter and the core and extended luminosities. The core-dominance parameter of galaxies is smaller than that in quasars, which is smaller than that in BL Lac objects. $\log R = -1.40 \pm 0.74$ for galaxies, $\log R = -0.53 \pm 0.92$ for quasars, and $\log R = 0.01 \pm 0.65$ for BL Lac objects on average respectively. For quasars, there is clear correlation between the core-luminosity and core-dominance parameter and an anti-correlation between the extended luminosity and the core-dominance parameter, which is explained by the beaming effect.

Key words. BL Lacertae objects: general – quasars: general – galaxies: Seyfert – galaxies: jets

1. Introduction

The relativistic beaming model has been successfully used to explain observational properties of active galactic nuclei (AGNs). In this model the emissions are composed of two components, namely, the boosted and the isotropic extended ones. The ratio of the two parts is defined as the core-dominance parameter (e.g., Orr & Brown 1982). Some authors used the ratio of flux densities but some others used the ratio of luminosities to indicate the core-dominance parameter (e.g., Punsly et al. 1995, and reference therein), so $R = \frac{S_c}{S_{Ext}}$ (or $R = \frac{L_c}{L_{Ext}}$). In the unified model, different viewing angles (the angle between the jet and the line of sight) give rise to different subclasses of objects, such as BL Lac objects (BLs), core-dominated quasars (CDQs), lobe-dominated quasars (LDQs), highly polarized quasars (HPQs), and superluminal sources (SLS) etc. BL Lacertae objects are presumed to be FRI type radio galaxies (Fanaroff & Riley 1974; Urry et al. 1991), but some evidence also suggests that the parent population of BL Lacs should be a mix of FRI and FRII (Kollgaard et al. 1996) and the extended radio morphologies of BLs were found to be of both FRI and II types (Kollgaard et al. 1992); some line emission from FRIIs is weak enough to be BL-like (Laing 1994), and from the Hubble relation point of view, the infrared magnitude of BLs, FRI and FRII(G) fit the same relation (Fan et al. 1997 and reference therein). Thus it may be appropriate to unify BL objects more generally with radio galaxies. Since emissions in jets are strongly beamed, the core-dominance parameter, R should indicate the orientation of the jet. Observations also show that optical polarization ($P_{opt}(\%)$)

is associated with R with high polarization corresponding to high R (Wills et al. 1992; Fan 2002a,b).

Some authors have investigated the relation between R and flux (or luminosities) or the luminosity properties from various samples. For instance, Punsly (1995) investigated the extended luminosity of strong radio cores for a sample of 134 ultraluminous radio core quasars. Those quasars have ultraluminous radio cores. (The core luminosity $P_c > 10^{46}$ erg s⁻¹ in the quasar rest frame from 10 MHz to 250 GHz.) Murphy et al. (1993) studied a complete sample of 89 powerful core-dominated radio sources (70 quasars, 19 BL Lacs) with core flux density, $S_c^{5\text{ GHz}} > 1$ Jy at 5 GHz. They visited the difference of core-dominance parameter, redshift, extend radio luminosity. Hough et al. (1989) defined a complete sample of 28 double-lobed radio quasars to make a statistical analysis of the large-scale structure to check for consistency with the beaming hypothesis in the central components. Hutchings et al. (1988), Neff et al. (1989), Neff & Hutchings (1990) studied a large sample of 250 core-dominated quasars. It was shown that the core dominance parameter increases with redshift. Very recently, a larger sample of 661 extragalactic radio sources were compiled and a relation between the 5 GHz core luminosity and 1.4 GHz total luminosity was discussed (Liu & Zhang 2002). From their paper we chose a sample of 542 sources with both core and total luminosities, and calculated their core-dominance parameters. The $\log R$ distribution and the correlation of luminosity and R are investigated. In Sect. 2, we give the sample and some results. In Sect. 3, we present some discussions and a brief summary.

2. Sample and results

2.1. Sample

From the paper by Liu & Zhang (2002), a sample of 542 objects with total luminosity (in W Hz^{-1}) at 1.4 GHz and core

Send offprint requests to: Dr. J. H. Fan,
e-mail: fjh@gzhu.edu.cn

[★] Table 1 is only available in electronic form at
<http://www.edpsciences.org>

luminosity at 5 GHz were chosen. Out of them, 27 are BL Lac objects, 300 are galaxies, and 215 are quasars. They are listed in Table 1, in which Col. 1 gives the source name, Col. 2 identification (BL stands for BL Lacertae objects, Q for quasars, G for radio galaxy, S0.5, S1, S2 and S3 for Seyfert galaxies), Col. 3 redshift, Col. 4 total luminosity at 1.4 GHz in units of W Hz^{-1} , Col. 5 core luminosity at 5 GHz in units of W Hz^{-1} , Col. 6 for core dominance parameter corresponding to $\alpha_E = 0.5$, and Col. 7 for core dominance parameter corresponding to $\alpha_E = 1.0$.

2.2. Result

To calculate the core-dominance parameter at 5 GHz, we assume that the core spectral index is $\alpha_C = 0.0$ ($S_\nu \propto \nu^{-\alpha}$), and the extended spectral index is $\alpha_E = 0.5$ and 1.0 respectively. Therefore, we have that the 1.4 GHz core luminosity is equal to the 5 GHz core luminosity, $P_{1.4 \text{ GHz}}^C = P_{5 \text{ GHz}}^C$, and the 1.4 GHz extended luminosity is the difference of the 1.4 GHz total and core luminosities, $P_{1.4 \text{ GHz}}^E = P_{1.4 \text{ GHz}}^T - P_{5 \text{ GHz}}^C$, considering the cosmic expansion, we have 5 GHz extended luminosity $P_E = P_{5 \text{ GHz}}^E(1+z)^{(\alpha_E-1)} = P_{1.4 \text{ GHz}}^E \times (1.4/5)^{\alpha_E}(1+z)^{(\alpha_E-1)}$. In this sense, the core-dominance parameter at 5 GHz is

$$R = \frac{P_C}{P_E} = \frac{P_{5 \text{ GHz}}^C}{P_{1.4 \text{ GHz}}^T - P_{5 \text{ GHz}}^C} (1.4/5)^{-\alpha_E} (1+z)^{-\alpha_E}. \quad (1)$$

The obtained results are listed in Cols. 6 and 7 for $\alpha_E = 0.5$ and 1.0 respectively. The corresponding distribution is also shown in Fig. 1.

2.2.1. R distribution

$\log R$ histogram of the whole sample are shown in Fig. 1 for the differently extended spectral index, α_E . The upper panel of Fig. 1 corresponds to $\alpha_E = 0.5$ while the lower panel to $\alpha_E = 1.0$. We found that the distribution of $\log R$ obtained from different extended spectral indices (α_E) is different. The steeper the spectrum the larger the R as shown in Fig. 1. If we consider different type of sources separately, we find that, on average, the core-dominance parameter of galaxies is smaller than that in quasars, which is smaller than that in BL Lac objects with the average $\log R$ for $\alpha_E = 0.5$ case being as follows: $\log R = -1.40 \pm 0.74$ for galaxies, $\log R = -0.53 \pm 0.92$ for quasars, and $\log R = 0.01 \pm 0.65$ for BL Lac objects respectively.

2.2.2. Relation between R and core and extended luminosities

From a statistical analysis, we consider the correlation between $\log R$ and $\log P_C$ and $\log P_E$ for the whole sample and individual sub-samples respectively. (Here we only take into account the $\alpha_E = 0.5$ case.) The corresponding diagrams are shown in Figs. 2 to 5. Relations between R and P_E and P_C for the whole sample are shown in Fig. 2. When a linear regression is applied to the data, we find a clear correlation between $\log R$ and $\log P_C$ for the whole sample, $\log P_C = (0.96 \pm 0.07) \log R + 25.34 \pm 0.10$ with a correlation coefficient $r = 0.50$ and a chance

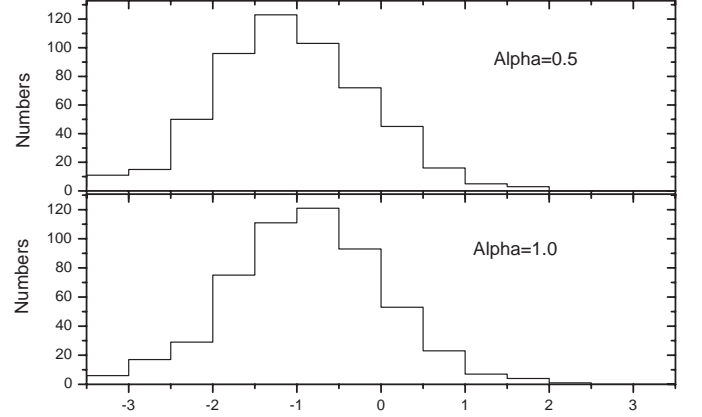


Fig. 1. Histogram of $\log R$ for the whole sample with differently extended spectral index. The upper panel corresponds to $\alpha_E = 0.5$, the lower panel to $\alpha_E = 1.0$.

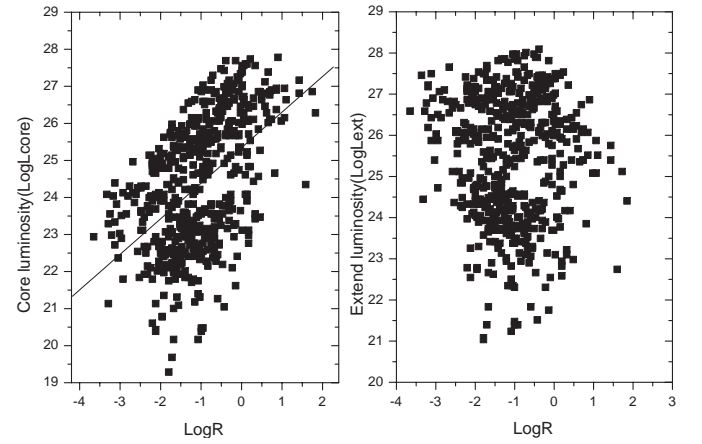


Fig. 2. Relation of luminosity and the core-dominance parameter (left panel is for core-luminosity and the straight line represents the best fit result and the right panel is for extended luminosity) for the whole sample.

probability $p \sim 0$. However, there is no clear relation for $\log R$ and $\log P_E$. We also consider the relation for different subclasses. The relation between R and P_E and P_C for quasars is shown in Fig. 3. There is a clear correlation between $\log R$ and $\log P_C$ for quasars, $\log P_C = (0.64 \pm 0.06) \log R + 26.4 \pm 0.06$ with a correlation coefficient $r = 0.59$ and a chance probability $p \sim 0$, and an anti-correlation for $\log R$ and $\log P_E$, $\log P_E = -(0.34 \pm 0.05) \log R + 26.43 \pm 0.06$ with a correlation coefficient $r = -0.39$ and a chance probability $p = 10^{-7}$. The relation between R and P_E and P_C for BL Lacs is shown in Fig. 4. There is no clear correlation between $\log R$ and $\log P_C$ or for $\log R$ and $\log P_E$ because of the small sample. The relation between R and P_E and P_C for galaxies is shown in Fig. 5. There is an anti-correlation between $\log R$ and $\log P_E$, $\log P_E = -(0.87 \pm 0.08) \log R + (23.26 \pm 0.14)$ with a correlation coefficient $r = -0.50$ and a chance probability $p \sim 0$, but there is no clear relation for $\log R$ and $\log P_C$.

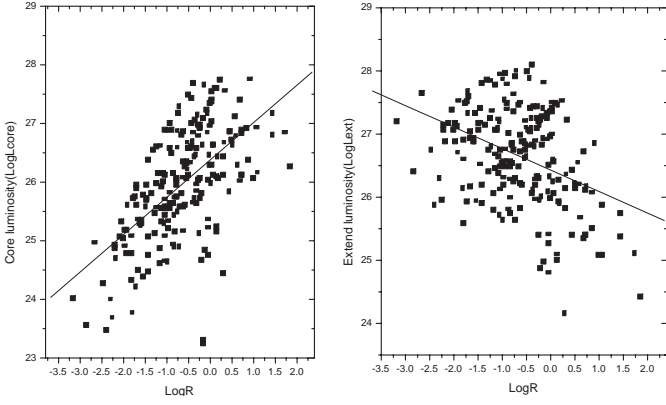


Fig. 3. Relation between luminosity and core-dominance parameter (left panel is for core-luminosity and the right panel is for extended luminosity) for quasars. The straight lines represent the best fit results.

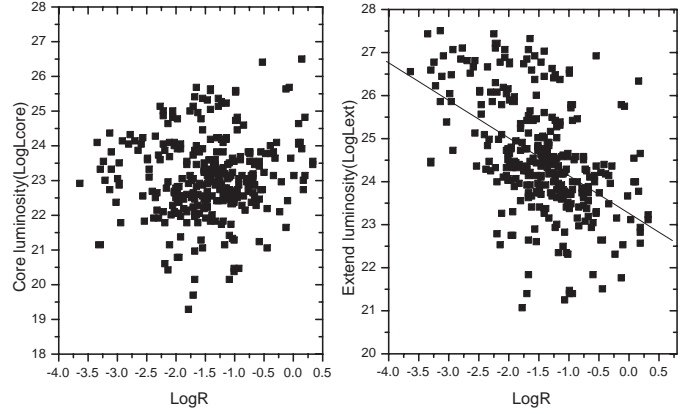


Fig. 5. Relation between luminosity and core-dominance parameter (left panel is for core-luminosity and the right panel is for extended luminosity, the straight line represents the best fit result) for galaxies.

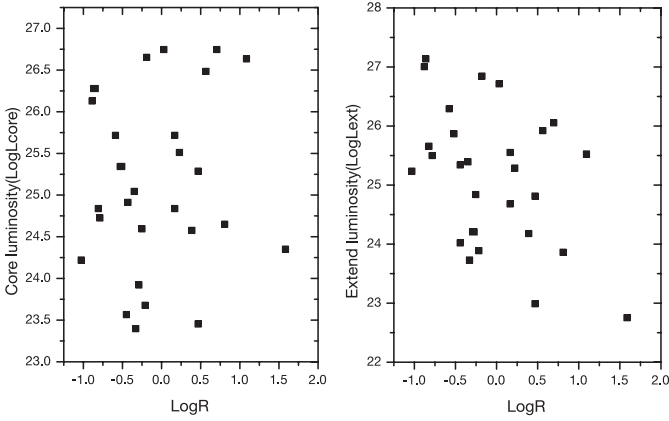


Fig. 4. Relation between luminosity and core-dominance parameter (left panel is for core-luminosity and the right panel is for extended luminosity) for BL Lacertae objects.

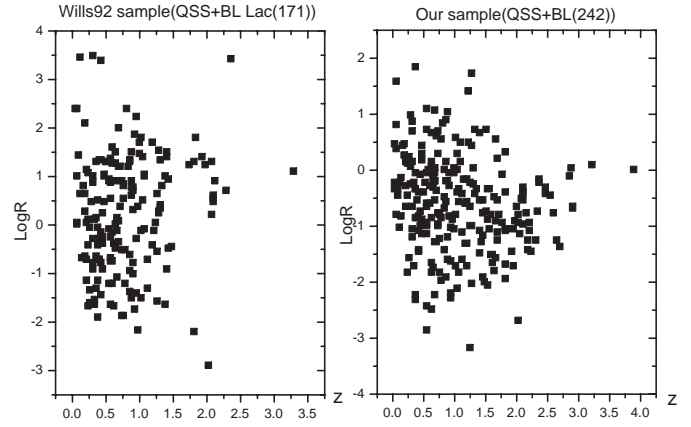


Fig. 6. Relation between the core-dominance parameter and redshift (left panel is for the data from Wills et al. (1992), and the right panel is from our results for BLs and quasars).

2.2.3. Relation between R and redshift

From relation (1), it is expected that there is a relation between redshift and core-dominance parameter, R , since $R = \frac{P_c}{P_E} = \frac{P_{5\text{GHz}}^c}{P_{1.4\text{GHz}}^c - P_{5\text{GHz}}^c} (1.4/5)^{-\alpha_E} (1+z)^{-\alpha_E}$. From our calculation and the known redshift, we find that there is no clear correlation between R and redshift (see Fig. 6).

3. Discussion

In extragalactic radio sources, the core-dominance parameter is taken as an orientation parameter. Wills et al. (1992) compiled a quasar sample. Ghisellini et al. (1993) also compiled a sample of extragalactic sources and found that the average $\log R$ in BL Lacs is larger than that in flat spectrum radio quasars (FSRQs). However, Murphy et al. (1993) obtained a distribution of $\log R$ for a core-dominated radio source sample (56 quasars, 18 BL Lacs) with the 5 GHz core flux densities being greater than 1 Jy. They found that there is a tendency for BL Lacs to have lower R than quasars in their sample. Although the difference is not significant, the results do not support the argument that BL Lacs are quasars with more highly beamed cores. Our present results show a tendency that the BL Lacs

have higher R than quasars, and that quasars have higher R than galaxies. This difference is illustrated by comparing their distribution of $\log R$ (Figs. 7, 9, 11) and cumulative probability (K-S test in Figs. 8, 10 and 12) for BL Lacs and galaxies, quasars and galaxies, BL Lacs and quasars respectively. The K-S test results indicate that the null hypothesis (they both are from the same parent population) cannot be rejected at the following confidence level for the different samples: $p = 0.003$ for BL Lacs and quasars, $p < 10^{-4}$ for BL Lacs and galaxies, and $p < 10^{-4}$ for quasars and galaxies. So, both BL Lacs and quasars are different from galaxies in this respect.

The R difference between different subclasses found here is consistent with that found by Ghisellini et al. (1993) but is in conflict with that found in Murphy et al. (1993). This difference is from the fact that Murphy et al. only considered bright sources ($S_{5\text{GHz}} > 1\text{Jy}$) while the sources considered in the paper by Ghisellini et al. (1993) and those in the present paper cover a large range of flux densities. Very recently, we found that the apparently higher R in BL Lacs than in FSRQs does not imply that the boosting factor (Doppler factor) in BL Lacs is greater than that in FSRQs. It is caused by the ratio of the intrinsic flux density in the jet to the extend flux density in the

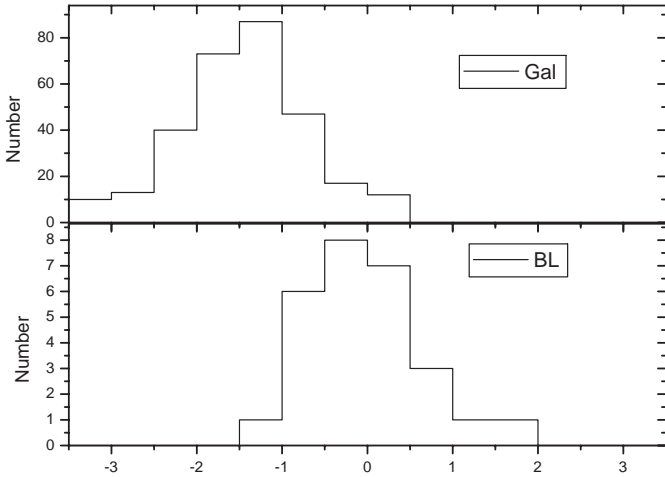


Fig. 7. Histogram comparison of core-dominance parameter for galaxies (upper panel) and BL Lacs (lower panel).

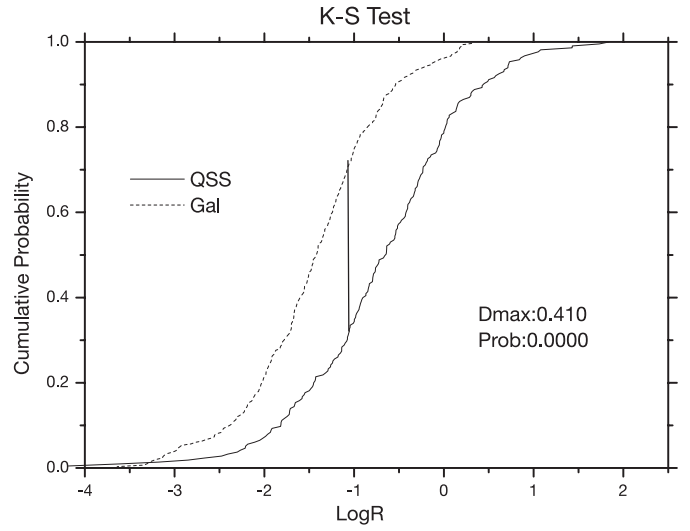


Fig. 10. K-S test for quasars and galaxies.

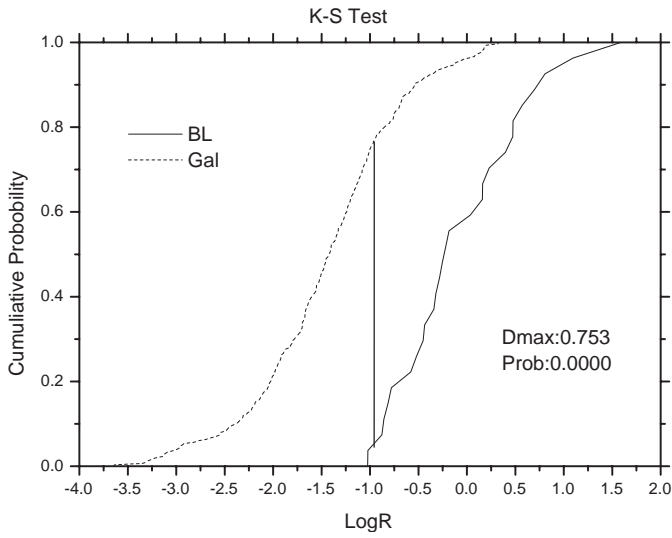


Fig. 8. K-S test for BL Lacs and galaxies.

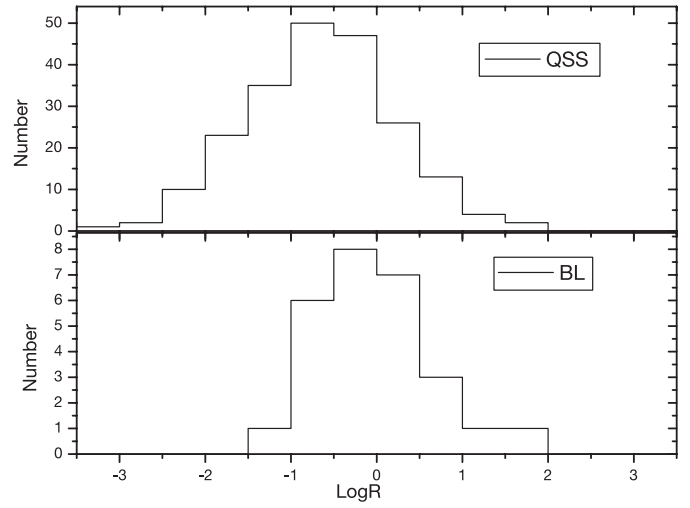


Fig. 11. Histogram comparison of core-dominance parameter for quasars (upper panel) and BL Lacs (lower panel).

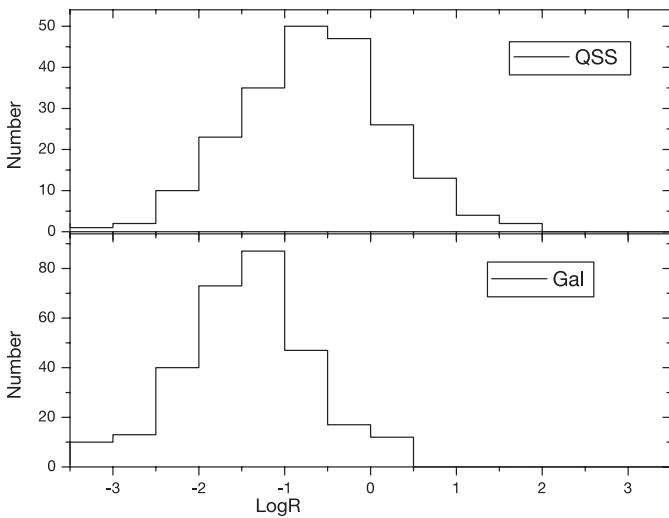


Fig. 9. Histogram comparison of core-dominance parameter for quasars (upper panel) and galaxies (lower panel).

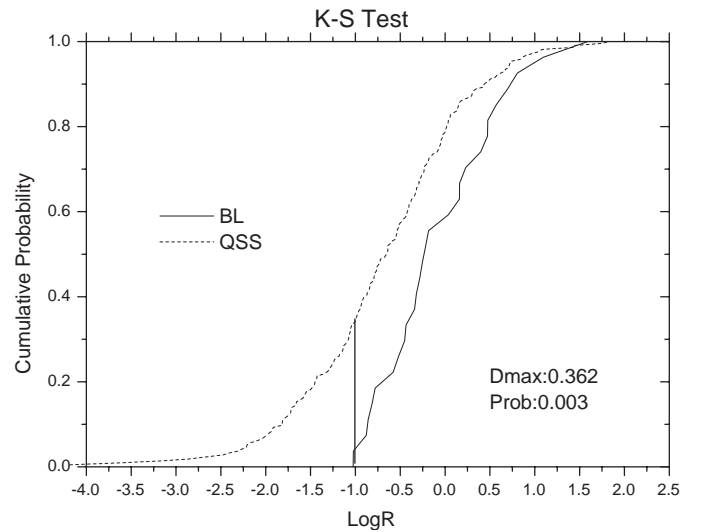


Fig. 12. K-S test for BL Lacs and quasars.

co-moving frame, $f = \frac{S_{\text{in}}^{\text{core}}}{S_{\text{in}}^{\text{ext}}}$, which is greater in BL Lacs than that in FSRQs, namely $f_{\text{BLs}} > f_{\text{FSRQs}}$. This difference in f between BLs and FSRQs can explain the emission line difference in BL Lacs and FSRQs (Fan 2002a,b, 2003).

3.1. Beaming model and R -luminosity relation for quasars

From Fig. 3, we have relations between $\log R$ and $\log P_C$ and $\log P_E$ for quasars. Similar correlations were also discussed in previous papers using various samples (Hough et al. 1989; Murphy et al. 1993; Punsly 1995). From their work, we found that $\log P_E$ is anti-correlated with $\log R$ for core-dominated radio quasars ($\log R > 0$), but there is no obvious correlation between $\log P_E$ and $\log R$ for lobe-dominated radio quasars ($\log R < 0$). No clear correlation can be found between $\log S_C$ (or $\log P_C$) and $\log R$ if we consider the data given in the papers by Murphy et al. (1993) and Punsly (1995). However, a clear correlation can be found between $\log S_C$ (or $\log P_C$) and $\log R$ if we consider the data given in the papers by Hough & Readhead (1989). Why is there such a contradiction? In fact, this different result can be explained using a beaming model as shown below. From a two-component beaming model, we have $R = \frac{P_C}{P_E}$, which is used in the following luminosity- R relation consideration.

Firstly, we consider the $\log R$ - $\log P_C$ relation. R can be expressed in a form

$$\frac{R}{1+R} = \frac{P_C}{P_E + P_C} = \frac{P_C}{P_T}$$

If P_T is a constant, then R is proportional to P_C when R is much smaller than unity, and there is no correlation between R and P_C when R is much greater than unity. Therefore, there is no $\log R$ - $\log P_C$ relation when R is large and there is $\log R$ - $\log P_C$ relation when R is small. When the data ($\log R < 0$ for all but two objects) by Hough & Readhead (1989) are considered, there is a clear correlation between $\log P_C$ and $\log R$. From the data in the present paper we have $\log P_T = 26.86 \pm 0.67$ for quasars. When we use $\log P_T = 26.86 + 0.67 = 27.53$ and $\log P_T = 26.86 - 0.67 = 26.19$, we can get two curves that show the relation between $\log P_C$ and $\log R$ as shown in Fig. 13. It is clear that most of the observation data are in between the area bounded by the two curves.

Secondly, we consider the $\log R$ - $\log P_E$ relation. R can be expressed in a form

$$1+R = \frac{P_C + P_E}{P_E} = \frac{P_T}{P_E}$$

If P_T is a constant, then $R+1$ is anti-proportional to P_E when R is much larger than unity, and there is no correlation between R and P_E when R is much smaller than unity. Therefore, there is no $\log R$ - $\log P_E$ relation when R is small and there is an anti-correlation of $\log R$ - $\log P_E$ when R is large. When the data ($\log R > 0.5$ for all sources) by Punsly (1995) are considered, a clear anti-correlation is seen between $\log P_E$ and $\log R$. When we use $\log P_T = 27.53$ and $\log P_T = 26.19$, we can get two curves to show the relation between $\log P_E$ and $\log R$ as shown

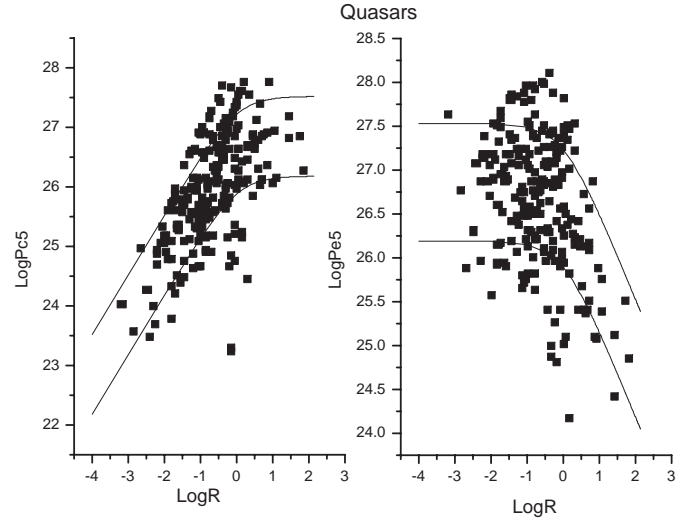


Fig. 13. Plot of luminosity against core-dominance parameter (left panel is for core-luminosity, the right panel is for extended luminosity) for quasars. The curves represent $\log P_T = 27.53 \text{ W Hz}^{-1}$ (upper curve) and $\log P_T = 26.19 \text{ W Hz}^{-1}$ (lower curve).

in Fig. 10, in which most of the observational data are in between the area bounded by the two curves.

3.2. Comparison with Wills et al. (1992)

From relation (1), there should be a correlation between R and redshift, but our calculation shown in Fig. 6 (right panel) does not show any correlation. This is probably from the fact that R in relation (1) does not only depends on redshift but also depend on a factor $\frac{P_C^{5 \text{ GHz}}}{P_T^{1.4 \text{ GHz}} - P_C^{5 \text{ GHz}}}$, which is different from one source to another and dilutes the R -redshift relation.

In 1992, Wills et al. compiled core-dominance parameters for a large sample of extragalactic sources including BL Lacs and quasars, and examined the R -redshift relation, but they found no clear R -redshift relation. For comparison, we consider their data in Fig. 6 (left panel). The two panels show similar results. Our result is consistent with that by Wills et al. (1992). Therefore, double jet radio sources (our results) and single jet radio sources show no difference in the R -redshift relation.

3.3. Summary

In the present paper, we calculated the core-dominance parameters (R) for a sample of 542 sources and compared the R values for different sub-samples (BL Lacs, Quasars, and galaxies). The average R in BL Lacs is larger than that in quasars, whose average R is greater than that in galaxies. We also investigated the correlation between R and luminosity. We found that there is a correlation between core-luminosity and R and an anti-correlation between extended luminosity and R for quasars. This relationship has been explained using a beaming model. Furthermore, there is no clear correlation between R and redshift for the whole sample or for individual sub-samples.

Acknowledgements. This work is partially supported by the National Natural Scientific Foundation of China(19973001), National 973

project (NKBRSF G19990754), the National Science Fund for Distinguished Young Scholars (10125313), and the Fund for Top Scholars of Guangdong Province (Q02114). The authors thank the referee, Dr. Rick Perley for the valuable comments and suggestions on this work.

References

- Browne, I. W. A., & Murphy, D. W. 1987, *MNRAS*, 226, 601
Fan, J. H. 2003, *ApJ*, 585, L23
Fan, J. H. 2002a, *PASJ*, 54, L55
Fan, J. H. 2002b, *IAU Symp.*, 214, August 5-10, Suzhou, China
Fan, J. H., Okudaira, A., Lin, R. G., & Xie, G. Z. 1997, *Ap&SS*, 253, 275
Fanaroff, B. L., & Riley, J. M. 1974, *MNRAS*, 167, 31
Ghisellini, G., Padovani, P., Celotti, A., & Maraschi, L. 1993, *ApJ*, 407, 65
Hough, D. H., & Readhead, A. C. S. 1989, *AJ*, 1208, 1225
Hutchings, J. B., Price, R., & Gower, A. 1988, *ApJ*, 329, 122
Kollgaard, R. I., Palma, C., Laurent-Muehleisen, S. A., & Feigelson, E. D. 1996, *ApJ*, 465, 115
Kollgaard, R. I., Wardle, J. F. C., Roberts, D. H., & Gabuzda, D. C. 1992, *AJ*, 104, 1687
Laing, R. A., Jenkins, C. R., Wall, J. V., & Unger, S. W. 1994, *ASP Conf. Ser.*, 54, 201
Liu, F. K., & Zhang, Y. H. 2002, *A&A*, 381, 757
Murphy, D. W., Browne, I. W. A., & Perley, R. A. 1993, *MNRAS*, 264, 298
Neff, S. G., Hutchings, J. B., & Gower, A. C. 1989, *AJ*, 97, 1291
Neff, S. G., & Hutchings, J. B. 1990, *AJ*, 100, 1441
Orr, M. J. L., & Brown, I. W. A. 1982, *MNRAS*, 200, 1067
Punsly, B. 1995, *AJ*, 109, 1555
Urry, C. M., Padovani, P., & Stickel, M. 1991, *ApJ*, 382, 501
Wills, B. J., Wills, D., Breger, M., Antonucci, R. R. J., & Barvainis, R. 1992, *ApJ*, 398, 454

Online Material

Table 1. Core-dominance parameters.

Name	ID	z	$\log P^T$	$\log P^C$	$\log R$	$\log R$	Name	ID	z	$\log P^T$	$\log P^C$	$\log R$	$\log R$
(1)	(2)	(3)	(4)	(5)	(6)	(7)	(1)	(2)	(3)	(4)	(5)	(6)	(7)
0414+009	BL	0.287	25.30	24.70	-0.20	0.08	0156-252	G	2.090	27.45	25.85	-1.31	-1.04
0521-365	BL	0.061	25.83	24.75	-0.77	-0.49	0157+393	G	0.072	24.34	23.66	-0.30	-0.03
0548-322	BL	0.069	24.39	23.60	-0.44	-0.16	0206+35	G	0.038	24.52	23.15	-1.07	-0.80
0723-008	BL	0.130	25.99	24.89	-0.79	-0.51	0211-122	G	2.336	27.30	25.30	-1.72	-1.44
0820+225	BL	0.951	27.47	26.42	-0.73	-0.46	0219+421	G	0.002	21.68	20.38	-1.00	-0.72
0826+180	BL	0.089	24.61	23.96	-0.26	0.01	0220+427	G	0.022	24.69	22.59	-1.82	-1.54
0828+493	BL	0.548	26.73	25.90	-0.48	-0.21	0234+315	G	1.575	27.08	23.72	-3.08	-2.81
0829+046	BL	0.180	25.55	25.35	0.51	0.79	0238+085	G	0.021	23.80	22.54	-0.96	-0.68
0954+658	BL	0.386	26.28	25.48	-0.45	-0.17	0247+467	G	0.029	23.97	22.56	-1.12	-0.84
1011+496	BL	0.200	25.25	24.91	0.20	0.48	0255+05	G	0.024	24.61	22.40	-1.93	-1.65
1101+384	BL	0.031	23.68	23.47	0.48	0.76	0256+132	G	0.075	24.07	22.30	-1.49	-1.21
1144+352	BL	0.063	24.39	24.37	1.60	1.88	0258+350	G	0.020	23.88	22.48	-1.11	-0.83
1156+295	BL	0.729	27.10	26.99	0.82	1.09	0300+162	G	0.032	24.52	21.94	-2.30	-2.03
1219+285	BL	0.100	25.56	24.26	-1.00	-0.72	0305+039	G	0.029	24.83	23.77	-0.74	-0.47
1400+162	BL	0.244	25.76	25.01	-0.39	-0.11	0313+683	G	0.090	24.92	23.56	-1.06	-0.79
1413+135	BL	0.249	25.91	25.61	0.28	0.55	0314+416	G	0.026	24.76	22.15	-2.33	-2.06
1511+103	BL	0.049	24.79	24.68	0.82	1.09	0319-454	G	0.063	25.26	22.82	-2.16	-1.89
1652+398	BL	0.034	24.30	23.69	-0.21	0.07	0320-37	G	0.006	24.73	21.15	-3.30	-3.03
1749+096	BL	0.322	26.16	25.83	0.22	0.50	0326+396	G	0.024	24.06	22.70	-1.06	-0.79
1749+701	BL	0.770	27.57	26.52	-0.73	-0.46	0327+246	G	0.106	23.71	22.71	-0.68	-0.40
1803+784	BL	0.680	27.34	26.97	0.15	0.42	0331-013	G	0.139	25.77	23.96	-1.53	-1.25
1807+698	BL	0.050	24.84	24.60	0.41	0.68	0335+096	G	0.035	23.70	22.36	-1.04	-0.77
1826+796	BL	0.664	27.39	26.88	-0.07	0.20	0336-35	G	0.005	22.82	20.41	-2.13	-1.86
2131-021	BL	0.557	26.87	26.82	1.19	1.47	0404+768	G	0.599	27.42	25.82	-1.31	-1.04
2200+420	BL	0.069	25.77	25.07	-0.33	-0.05	0405-123	G	0.574	27.39	26.60	-0.44	-0.16
2201+044	BL	0.028	24.10	23.41	-0.31	-0.04	0406-244	G	2.440	27.64	25.41	-1.95	-1.67
2240-260	BL	0.774	26.87	26.73	0.70	0.97	0411+141	G	0.206	26.51	24.17	-2.06	-1.79
0007+106	G	0.090	25.33	23.85	-1.19	-0.91	0417-181	G	2.773	27.63	24.72	-2.63	-2.36
0007+124	G	0.110	25.41	22.74	-2.39	-2.12	0439+083	G	0.152	25.07	23.12	-1.67	-1.39
0015-229	G	2.010	27.42	25.32	-1.82	-1.54	0445+44	G	0.021	24.58	21.92	-2.38	-2.11
0019+230	G	0.134	24.63	22.67	-1.68	-1.40	0448+520	G	0.109	26.79	23.57	-2.94	-2.67
0031+060	G	0.133	24.71	22.48	-1.95	-1.67	0449-175	G	0.031	23.97	22.03	-1.66	-1.38
0034+254	G	0.032	23.13	21.77	-1.06	-0.79	0457+052	G	0.098	24.48	22.97	-1.22	-0.94
0034-014	G	0.073	25.41	23.48	-1.65	-1.37	0457+054	G	0.054	23.71	21.81	-1.62	-1.34
0035+180	G	0.145	24.70	23.27	-1.14	-0.86	0459+252	G	0.278	26.72	25.33	-1.10	-0.82
0039+211	G	0.102	24.89	23.60	-0.99	-0.71	0518-458	G	0.034	25.93	24.01	-1.64	-1.36
0040+517	G	0.174	26.52	23.07	-3.17	-2.90	0546-329	G	0.147	25.47	23.90	-1.28	-1.01
0043+201	G	0.106	25.06	23.07	-1.71	-1.43	0658+329	G	0.127	24.78	22.87	-1.63	-1.35
0047+241	G	0.082	24.17	23.08	-0.78	-0.50	0658+330	G	0.127	24.98	23.68	-1.00	-0.72
0050-220	G	0.059	23.57	22.98	-0.18	0.09	0702+749	G	0.292	26.41	24.00	-2.13	-1.86
0053+260	G	0.192	25.04	23.00	-1.76	-1.48	0704+351	G	0.078	24.28	21.83	-2.17	-1.90
0053-016	G	0.042	24.34	22.19	-1.87	-1.59	0712+534	G	0.064	24.83	22.96	-1.59	-1.31
0055+265	G	0.047	24.61	22.29	-2.04	-1.77	0720+381	G	0.220	25.24	24.92	0.24	0.52
0055-016	G	0.045	25.10	23.32	-1.50	-1.22	0720+670	G	0.086	23.85	23.58	0.34	0.62
0104+321	G	0.017	24.21	22.45	-1.48	-1.20	0733+597	G	0.040	23.99	22.93	-0.74	-0.47
0108-146	G	0.103	24.60	23.80	-0.45	-0.17	0738+441	G	0.117	24.92	23.86	-0.74	-0.47
0110+152	G	0.048	24.34	22.06	-2.00	-1.72	0745+521	G	0.068	24.42	22.68	-1.46	-1.18
0114-476	G	0.146	25.87	23.16	-2.43	-2.16	0755+379	G	0.041	24.49	23.59	-0.57	-0.29
0123-016	G	0.019	24.38	22.02	-2.08	-1.81	0756+272	G	0.096	24.66	22.68	-1.70	-1.42
0124+189	G	0.042	24.42	22.59	-1.55	-1.27	0757+395	G	0.057	23.60	23.16	0.03	0.31
0128+002	G	0.103	24.82	23.13	-1.40	-1.13	0821+695	G	0.538	25.70	24.36	-1.04	-0.77
0136+185	G	0.069	23.92	22.44	-1.19	-0.91	0824+294	G	0.458	26.73	24.96	-1.49	-1.21
0136+396	G	0.211	25.76	24.29	-1.18	-0.90	0828+193	G	2.572	26.97	25.68	-0.99	-0.71
0139+073	G	0.062	23.26	22.31	-0.62	-0.35	0831+557	G	0.240	26.97	25.45	-1.23	-0.95
0141+061	G	0.089	24.04	22.25	-1.51	-1.23	0836+290	G	0.065	24.73	23.86	-0.53	-0.25
0149+358	G	0.016	22.62	21.31	-1.01	-0.74	0838+325	G	0.069	24.51	24.13	0.13	0.41

Table 1. continued.

Name	ID	z	$\log P^T$	$\log P^C$	$\log R$	$\log R$	Name	ID	z	$\log P^T$	$\log P^C$	$\log R$	$\log R$
(1)	(2)	(3)	(4)	(5)	(6)	(7)	(1)	(2)	(3)	(4)	(5)	(6)	(7)
0844+319	G	0.068	24.88	23.35	-1.24	-0.96	1256+281	G	0.024	22.91	21.08	-1.55	-1.27
0844+540	G	0.045	24.56	22.59	-1.69	-1.41	1257+28	G	0.023	23.05	20.81	-1.96	-1.68
0902+343	G	3.395	27.94	26.33	-1.32	-1.05	1258-321	G	0.017	23.53	22.54	-0.67	-0.39
0905-097	G	0.054	24.15	23.16	-0.67	-0.39	1306+107	G	0.136	24.33	23.12	-0.91	-0.63
0907-091	G	0.138	24.24	23.26	-0.66	-0.38	1308-441	G	0.051	24.55	23.81	-0.38	-0.10
0908+376	G	0.105	24.89	23.50	-1.10	-0.82	1313+073	G	0.051	24.75	22.57	-1.90	-1.62
0908-103	G	0.129	25.06	23.39	-1.38	-1.11	1316+299	G	0.073	24.85	23.25	-1.31	-1.04
0909+162	G	0.085	24.17	21.99	-1.90	-1.62	1318-434	G	0.011	23.87	22.88	-0.67	-0.39
0910+411	G	0.442	24.51	23.60	-0.58	-0.30	1319+428	G	0.079	25.27	22.69	-2.30	-2.03
0913+38	G	0.071	24.27	22.48	-1.51	-1.23	1320+584	G	0.193	25.15	23.56	-1.30	-1.03
0915+32	G	0.062	24.00	22.56	-1.15	-0.87	1321+31	G	0.016	23.85	21.77	-1.80	-1.52
0936-041	G	0.094	24.70	23.16	-1.25	-0.97	1322+36	G	0.018	23.42	22.38	-0.72	-0.45
1004+146	G	0.031	24.07	22.97	-0.79	-0.51	1322-427	G	0.001	24.62	22.12	-2.22	-1.95
1005+28	G	0.148	24.25	22.60	-1.36	-1.09	1333-337	G	0.081	25.23	23.61	-1.33	-1.06
1009+748	G	0.810	27.27	24.31	-2.68	-2.41	1335+047	G	0.013	24.41	22.46	-1.67	-1.39
1010+350	G	1.414	27.14	26.87	0.34	0.62	1336+39	G	0.246	26.39	23.85	-2.26	-1.99
1029+570	G	0.034	23.81	22.50	-1.01	-0.74	1343-601	G	0.012	25.20	23.58	-1.33	-1.06
1040+31	G	0.036	24.03	22.77	-0.96	-0.68	1350+316	G	0.045	25.01	22.70	-2.03	-1.76
1100+358	G	1.440	27.06	25.35	-1.43	-1.15	1355+219	G	0.067	23.74	23.47	0.34	0.62
1101-325	G	0.355	26.28	25.82	0.00	0.28	1357+28	G	0.063	24.03	22.45	-1.29	-1.02
1102+30	G	0.072	24.29	22.76	-1.24	-0.96	1359-113	G	0.037	24.49	23.08	-1.12	-0.84
1107-372	G	0.010	22.80	21.42	-1.09	-0.81	1400-001	G	2.363	27.29	25.51	-1.50	-1.22
1108+27	G	0.033	23.01	22.21	-0.45	-0.17	1407+177	G	0.016	23.68	22.00	-1.39	-1.12
1108+411	G	0.074	24.73	22.91	-1.54	-1.26	1414+110	G	0.024	24.43	22.69	-1.46	-1.18
1113+295	G	0.049	24.67	22.94	-1.45	-1.17	1415+084	G	0.057	24.08	22.28	-1.52	-1.24
1113-178	G	2.239	27.39	25.66	-1.45	-1.17	1420+198	G	0.272	26.44	23.74	-2.42	-2.15
1116+28	G	0.067	24.33	23.17	-0.85	-0.58	1422+26	G	0.037	24.00	22.25	-1.47	-1.19
1120+013	G	0.072	24.12	22.65	-1.18	-0.90	1441+522	G	0.140	25.05	23.44	-1.32	-1.05
1122+390	G	0.007	21.76	20.46	-1.00	-0.72	1448+634	G	0.041	24.73	22.57	-1.88	-1.60
1130-037	G	0.063	24.54	23.85	-0.31	-0.04	1450+28	G	0.127	24.56	22.56	-1.72	-1.44
1131+493	G	0.032	24.13	22.74	-1.10	-0.82	1452-517	G	0.016	23.75	22.68	-0.75	-0.48
1132+492	G	0.032	23.73	22.59	-0.83	-0.55	1453+120	G	0.032	23.65	22.77	-0.54	-0.27
1137+18	G	0.011	23.06	20.59	-2.19	-1.92	1508+059	G	0.077	25.13	22.52	-2.33	-2.06
1138-262	G	2.156	27.73	25.49	-1.96	-1.68	1508+065	G	0.082	24.61	22.98	-1.34	-1.07
1141+354	G	1.781	27.15	24.73	-2.14	-1.87	1518+045	G	0.052	24.91	23.85	-0.74	-0.47
1146+596	G	0.011	23.71	21.93	-1.50	-1.22	1521+288	G	0.083	24.58	23.58	-0.68	-0.40
1155+266	G	0.112	25.10	22.87	-1.95	-1.67	1525+290	G	0.065	23.98	22.10	-1.60	-1.32
1159+583	G	0.102	25.07	22.81	-1.98	-1.70	1528+29	G	0.084	24.21	22.31	-1.62	-1.34
1201+282	G	0.139	24.68	21.89	-2.51	-2.24	1553+24	G	0.043	23.36	23.01	0.18	0.46
1209+746	G	0.107	24.99	23.26	-1.45	-1.17	1603+001	G	0.059	24.91	23.27	-1.35	-1.08
1216+061	G	0.007	24.01	22.25	-1.48	-1.20	1603+178	G	0.032	23.93	21.97	-1.68	-1.40
1222+13	G	0.003	23.24	21.72	-1.23	-0.95	1607+268	G	0.473	26.99	25.78	-0.91	-0.63
1227+119	G	0.084	25.12	23.34	-1.50	-1.22	1610-608	G	0.014	23.97	22.41	-1.27	-1.00
1231+674	G	0.106	25.06	22.85	-1.93	-1.65	1613+27	G	0.065	24.03	22.69	-1.04	-0.77
1233+168	G	0.078	24.96	22.68	-2.00	-1.72	1615+351	G	0.030	23.40	22.48	-0.59	-0.31
1233+169	G	0.078	24.64	23.60	-0.72	-0.45	1615+425	G	0.131	24.20	23.20	-0.68	-0.40
1234-723	G	0.023	23.87	23.16	-0.34	-0.06	1621+380	G	0.031	23.62	22.75	-0.53	-0.25
1238+188	G	0.072	24.48	22.88	-1.31	-1.04	1623+410	G	0.030	23.11	22.76	0.18	0.46
1243+267	G	0.089	24.22	22.81	-1.12	-0.84	1626+278	G	0.448	26.80	23.49	-3.03	-2.76
1244+699	G	0.157	24.80	23.25	-1.26	-0.98	1626+396	G	0.030	24.51	23.16	-1.05	-0.78
1247-012	G	0.083	24.34	23.45	-0.55	-0.28	1636+379	G	0.161	25.26	23.12	-1.86	-1.58
1250-102	G	0.014	23.27	22.14	-0.82	-0.54	1637+299	G	0.088	24.40	22.89	-1.22	-0.94
1251+273	G	0.027	23.55	21.16	-2.11	-1.84	1638+32	G	0.140	24.80	24.06	-0.38	-0.10
1252-122	G	0.086	25.38	22.99	-2.11	-1.84	1641+399	G	0.110	24.93	23.21	-1.44	-1.16
1253-055	G	0.014	24.23	22.13	-1.82	-1.54	1643+27	G	0.102	24.05	22.74	-1.01	-0.74
1254+277	G	0.025	22.63	21.18	-1.16	-0.88	1648+050	G	0.154	27.10	23.61	-3.21	-2.94

Table 1. continued.

Name	ID	z	$\log P^T$	$\log P^C$	$\log R$	$\log R$	Name	ID	z	$\log P^T$	$\log P^C$	$\log R$	$\log R$
(1)	(2)	(3)	(4)	(5)	(6)	(7)	(1)	(2)	(3)	(4)	(5)	(6)	(7)
1658+30A	G	0.035	23.88	22.89	-0.67	-0.39	0710+439	S	0.518	27.15	24.82	-2.05	-1.78
1658+326	G	0.102	24.52	22.62	-1.62	-1.34	1005+449	S	0.880	27.92	24.65	-2.99	-2.72
1709+460	G	0.056	23.32	21.84	-1.19	-0.91	1142+198	S	0.021	24.48	23.09	-1.10	-0.82
1712+638	G	0.806	27.23	24.39	-2.56	-2.29	1358+624	S	0.431	27.01	24.22	-2.51	-2.24
1736+32	G	0.074	24.14	22.92	-0.92	-0.64	1416+423	S0.5	0.017	21.86	21.07	-0.44	-0.16
1743+666	G	0.272	25.58	23.55	-1.75	-1.47	0055+300	S1	0.017	24.08	23.24	-0.50	-0.22
1747+30	G	0.130	23.96	22.91	-0.73	-0.46	0106+729	S1	0.181	26.11	23.76	-2.07	-1.80
1752+32B	G	0.045	23.47	22.30	-0.86	-0.59	0240-002	S1	0.004	22.94	20.99	-1.67	-1.39
1753+580	G	0.160	24.62	23.32	-1.00	-0.72	0309+390	S1	0.161	25.72	24.31	-1.12	-0.84
1759+211	G	0.080	24.78	23.11	-1.38	-1.11	0410+110	S1	0.307	26.80	25.15	-1.36	-1.09
1815+680	G	0.230	25.09	24.71	0.13	0.41	0415+379	S1	0.049	26.29	24.47	-1.54	-1.26
1819+396	G	0.400	26.85	25.40	-1.16	-0.88	0511+008	S1	0.127	25.69	22.41	-3.00	-2.73
1823+568	G	0.088	24.84	23.65	-0.88	-0.61	0549-074	S1	0.007	22.18	21.63	-0.13	0.15
1827+32	G	0.066	24.07	23.08	-0.67	-0.39	0609+710	S1	0.014	23.54	21.85	-1.40	-1.13
1829+290	G	0.842	27.47	25.26	-1.93	-1.65	0645+744	S1	0.019	23.03	20.81	-1.94	-1.66
1834+620	G	0.519	26.45	23.78	-2.39	-2.12	0917+458	S1	0.174	26.45	24.18	-1.99	-1.71
1842+455	G	0.091	25.73	23.76	-1.69	-1.41	0958+290	S1	0.185	26.30	24.14	-1.88	-1.60
1850+702	G	0.079	24.32	23.96	0.17	0.44	1208+396	S1	0.003	21.71	20.47	-0.94	-0.66
1919+479	G	0.103	25.22	23.19	-1.75	-1.47	1223+129	S1	0.008	22.11	20.16	-1.67	-1.39
1939+605	G	0.201	26.37	24.09	-2.00	-1.72	1447+771	S1	0.141	25.75	24.53	-0.92	-0.64
1940+50	G	0.025	24.31	22.08	-1.95	-1.67	1833+326	S1	0.058	25.34	23.63	-1.43	-1.15
1946+708	G	0.101	25.03	23.26	-1.49	-1.21	1845+797	S1	0.057	25.59	24.10	-1.20	-0.92
2025-218	G	2.630	27.65	24.88	-2.49	-2.22	2005-044	S1	0.057	27.73	24.12	-3.33	-3.06
2036-254	G	2.000	27.42	24.29	-2.85	-2.58	2116+818	S1	0.086	24.51	24.11	0.10	0.37
2045+068	G	0.127	25.67	23.60	-1.79	-1.51	2223-052	S1	0.057	25.30	23.51	-1.51	-1.23
2105+236	G	2.479	27.63	25.94	-1.40	-1.13	0116+082	S2	0.594	27.18	25.54	-1.35	-1.08
2116+26	G	0.016	22.72	22.10	-0.22	0.05	0256+366	S2	0.012	22.18	21.26	-0.59	-0.31
2128+048	G	0.990	27.85	25.46	-2.11	-1.84	0328-033	S2	0.020	21.55	20.18	-1.07	-0.80
2141+279	G	0.215	26.21	23.99	-1.94	-1.66	0356+102	S2	0.031	25.02	21.81	-2.93	-2.66
2148-555	G	0.035	26.14	22.91	-2.95	-2.68	0651+542	S2	0.238	26.35	23.13	-2.94	-2.67
2149-158	G	0.062	24.26	22.80	-1.17	-0.89	0714-292	S2	0.005	21.34	19.28	-1.78	-1.50
2152+085	G	0.150	24.77	23.28	-1.20	-0.92	0806-103	S2	0.110	25.73	23.88	-1.57	-1.29
2152-699	G	0.028	25.82	23.86	-1.68	-1.40	0836+299	S2	0.064	24.51	22.97	-1.25	-0.97
2153+377	G	0.292	26.86	23.99	-2.59	-2.32	1030+602	S2	0.051	22.67	21.35	-1.02	-0.75
2202+128	G	2.704	27.37	24.82	-2.27	-2.00	1201+205	S2	0.024	23.58	21.38	-1.92	-1.64
2203+292	G	0.708	26.96	23.16	-3.52	-3.25	1216+423	S2	0.002	21.68	19.70	-1.70	-1.42
2212+136	G	0.027	24.41	22.10	-2.03	-1.76	1244+492	S2	0.206	25.84	24.30	-1.25	-0.97
2229+391	G	0.017	24.02	22.07	-1.67	-1.39	1345+125	S2	0.121	26.10	24.87	-0.93	-0.65
2229-086	G	0.073	24.68	23.23	-1.16	-0.88	1529+242	S2	0.096	26.15	23.62	-2.25	-1.98
2236+35	G	0.028	23.44	21.83	-1.32	-1.05	1559+021	S2	0.104	26.10	23.39	-2.43	-2.16
2236-176	G	0.070	24.96	22.71	-1.97	-1.69	1637+826	S2	0.023	24.14	23.66	-0.03	0.25
2243+394	G	0.081	25.90	24.23	-1.38	-1.11	1642+690	S2	0.160	26.05	24.81	-0.94	-0.66
2243-178	G	0.123	24.89	23.28	-1.32	-1.05	1949+023	S2	0.059	25.41	22.59	-2.54	-2.27
2259+137	G	0.172	24.91	23.74	-0.86	-0.59	2121+248	S2	0.102	26.15	22.76	-3.11	-2.84
2308+072	G	0.045	24.75	24.10	-0.26	0.01	0238-084	S3	0.005	22.96	22.43	-0.10	0.17
2309+184	G	0.428	26.64	24.21	-2.15	-1.88	0915-118	S3	0.053	26.14	23.95	-1.91	-1.63
2316+184	G	0.040	23.70	22.41	-0.99	-0.71	1003+351	S3	0.099	25.78	24.64	-0.83	-0.55
2318+079	G	0.011	23.17	21.31	-1.58	-1.30	0007+332	Q	0.743	26.55	24.57	-1.70	-1.42
2322+143	G	0.044	24.22	22.25	-1.69	-1.41	0017+154	Q	2.012	28.16	25.45	-2.43	-2.16
2330+091	G	0.162	24.82	22.56	-1.98	-1.70	0017+257	Q	0.284	26.62	26.23	0.11	0.39
2335+267	G	0.029	24.85	23.37	-1.19	-0.91	0017-207	Q	0.545	26.26	23.67	-2.31	-2.04
2337+268	G	0.031	23.49	23.15	0.20	0.48	0022-297	Q	0.406	26.75	25.45	-1.00	-0.72
2352+495	G	0.238	26.26	25.74	-0.09	0.19	0033+079	Q	1.578	27.08	26.16	-0.59	-0.31
2354+471	G	0.046	24.63	22.49	-1.86	-1.58	0033+183	Q	1.469	27.65	25.58	-1.79	-1.51
2357+004	G	0.084	25.32	23.65	-1.38	-1.11	0035+121	Q	1.395	27.67	26.97	-0.33	-0.05
2210+016	G?	0.500	26.92	25.72	-0.90	-0.62	0038-019	Q	1.690	27.63	26.44	-0.88	-0.61

Table 1. continued.

Name	ID	z	$\log P^T$	$\log P^C$	$\log R$	$\log R$	Name	ID	z	$\log P^T$	$\log P^C$	$\log R$	$\log R$
(1)	(2)	(3)	(4)	(5)	(6)	(7)	(1)	(2)	(3)	(4)	(5)	(6)	(7)
0048+509	Q	0.937	27.30	24.98	-2.04	-1.77	0836+195	Q	1.691	27.24	26.56	-0.30	-0.03
0051+291	Q	1.828	27.47	26.90	-0.16	0.12	0836+710	Q	2.160	28.51	27.67	-0.50	-0.22
0109+200	Q	0.746	26.97	25.98	-0.67	-0.39	0838+133	Q	0.684	27.23	26.45	-0.42	-0.15
0110+297	Q	0.363	26.13	25.04	-0.78	-0.50	0839+186	Q	1.272	27.39	27.23	0.63	0.90
0127+233	Q	1.460	28.01	26.01	-1.72	-1.44	0839+616	Q	0.862	27.13	25.06	-1.79	-1.51
0130+24	Q	0.457	26.21	25.11	-0.79	-0.51	0850+140	Q	1.110	27.52	26.27	-0.95	-0.67
0133+207	Q	0.425	26.89	25.23	-1.37	-1.10	0850+581	Q	1.322	27.35	27.26	0.91	1.19
0134+329	Q	0.367	27.42	25.00	-2.14	-1.87	0855+143	Q	1.049	27.61	25.38	-1.95	-1.67
0138+136	Q	0.620	27.14	24.49	-2.37	-2.10	0859+470	Q	1.462	28.17	27.27	-0.57	-0.29
0153+744	Q	2.338	28.62	27.81	-0.46	-0.18	0859+681	Q	1.499	27.33	27.24	0.91	1.19
0202+149	Q	0.833	27.61	27.23	0.13	0.41	0859-140	Q	1.330	27.99	27.36	-0.24	0.04
0212+735	Q	2.367	28.59	28.20	0.11	0.39	0903+169	Q	0.411	26.27	24.63	-1.35	-1.08
0221+067	Q	0.511	26.81	26.25	-0.14	0.13	0906+430	Q	0.668	27.37	26.86	-0.07	0.20
0229+341	Q	1.238	27.65	24.37	-3.00	-2.73	0919+218	Q	1.421	27.24	25.85	-1.10	-0.82
0238+100	Q	1.816	27.29	26.16	-0.82	-0.54	0937+391	Q	0.617	26.55	24.71	-1.56	-1.28
0307+444	Q	1.165	27.40	26.61	-0.44	-0.16	0938+39	Q	0.618	26.99	25.00	-1.71	-1.43
0317-023	Q	2.092	27.68	27.09	-0.18	0.09	0941+261	Q	2.910	28.12	27.39	-0.36	-0.09
0333+321	Q	1.258	28.36	27.23	-0.82	-0.54	0941+522	Q	0.565	26.57	26.17	0.10	0.37
0400+258	Q	2.109	28.53	27.51	-0.70	-0.42	0953+254	Q	0.712	26.66	26.53	0.73	1.01
0409+229	Q	1.215	27.21	27.06	0.66	0.94	0957+003	Q	0.907	27.03	26.02	-0.69	-0.41
0411+055	Q	2.639	28.43	27.17	-0.96	-0.68	0957+561	Q	1.405	27.15	25.96	-0.88	-0.61
0420-014	Q	0.915	27.82	27.26	-0.14	0.13	1001+226	Q	0.974	26.94	25.73	-0.91	-0.63
0429+415	Q	1.023	28.11	26.26	-1.57	-1.29	1004+130	Q	0.240	25.91	23.87	-1.76	-1.48
0437-244	Q	0.840	26.61	25.02	-1.30	-1.03	1007+417	Q	0.613	26.91	25.85	-0.74	-0.47
0445+097	Q	2.110	27.78	27.29	-0.04	0.23	1015+359	Q	1.226	27.18	27.16	1.60	1.88
0454-220	Q	0.530	26.89	25.74	-0.84	-0.57	1018+456	Q	0.364	25.34	24.89	0.02	0.29
0504+030	Q	2.453	28.11	27.54	-0.16	0.12	1020+400	Q	1.254	27.51	26.70	-0.46	-0.18
0518+165	Q	0.759	27.79	26.40	-1.10	-0.82	1022+194	Q	0.828	27.32	26.60	-0.35	-0.08
0528+134	Q	2.070	28.62	27.97	-0.26	0.01	1023+067	Q	1.699	27.38	26.47	-0.58	-0.30
0537+531	Q	1.275	27.22	27.21	1.91	2.19	1028+313	Q	0.177	24.80	24.52	0.32	0.60
0538+498	Q	0.545	27.95	26.78	-0.86	-0.59	1032+343	Q	0.680	25.87	25.45	0.06	0.34
0548+165	Q	0.474	26.85	25.50	-1.05	-0.78	1038+528	Q	0.677	26.44	26.39	1.19	1.47
0553-205	Q	1.544	26.81	26.26	-0.13	0.15	1040+123	Q	1.029	27.80	27.16	-0.25	0.03
0605-085	Q	0.870	27.86	27.37	-0.04	0.23	1055+201	Q	1.111	27.65	27.01	-0.25	0.03
0637-752	Q	0.654	27.84	27.40	0.03	0.31	1058+726	Q	0.375	26.43	25.79	-0.25	0.03
0707+476	Q	1.310	27.81	27.30	-0.07	0.20	1100+772	Q	0.311	26.41	25.00	-1.12	-0.84
0710+118	Q	0.768	27.28	25.16	-1.84	-1.56	1103-006	Q	0.426	26.39	25.32	-0.75	-0.48
0711+356	Q	1.626	27.99	26.14	-1.57	-1.29	1104+167	Q	0.632	26.61	26.30	0.26	0.54
0723+679	Q	0.846	27.39	26.62	-0.41	-0.14	1107+483	Q	0.740	26.70	25.73	-0.64	-0.37
0730+257	Q	2.686	27.73	26.37	-1.06	-0.79	1136-135	Q	0.554	27.15	26.27	-0.54	-0.27
0740+380	Q	1.060	27.34	25.40	-1.66	-1.38	1137+660	Q	0.646	27.90	25.98	-1.64	-1.36
0740+828	Q	1.991	28.10	27.34	-0.40	-0.12	1142+052	Q	1.342	27.50	26.94	-0.14	0.13
0742+318	Q	0.462	26.55	26.24	0.26	0.54	1150+497	Q	0.334	26.43	25.85	-0.17	0.11
0745+241	Q	0.410	26.56	25.88	-0.30	-0.03	1150+812	Q	1.250	27.76	27.26	-0.06	0.22
0748+126	Q	0.889	27.26	27.21	1.19	1.47	1158+122	Q	2.018	27.14	26.13	-0.69	-0.41
0751+298	Q	2.106	27.47	26.80	-0.29	-0.01	1206+439	Q	1.400	27.66	26.08	-1.29	-1.02
0752+258	Q	0.446	26.03	24.81	-0.92	-0.64	1217+023	Q	0.240	25.68	25.33	0.18	0.46
0758+143	Q	1.200	27.78	25.95	-1.55	-1.27	1222+216	Q	0.435	26.64	26.19	0.02	0.29
0800+608	Q	0.689	26.82	25.35	-1.18	-0.90	1225+368	Q	1.975	28.36	27.37	-0.67	-0.39
0802+103	Q	1.956	28.12	26.36	-1.48	-1.20	1226+023	Q	0.158	27.14	26.92	0.46	0.73
0805+046	Q	2.877	27.90	27.62	0.32	0.60	1226+105	Q	2.296	27.81	26.51	-1.00	-0.72
0812+02	Q	0.402	26.68	25.60	-0.77	-0.49	1235-182	Q	2.192	27.34	26.33	-0.69	-0.41
0812+367	Q	1.025	27.23	27.10	0.73	1.01	1241+166	Q	0.557	27.08	25.74	-1.04	-0.77
0821+621	Q	0.542	26.42	26.31	0.82	1.09	1250+568	Q	0.320	26.61	25.70	-0.58	-0.30
0833+654	Q	1.112	27.39	25.69	-1.41	-1.14	1258+404	Q	1.659	27.84	26.21	-1.34	-1.07
0835+580	Q	1.536	27.86	25.73	-1.85	-1.57	1303-250	Q	0.738	26.63	25.46	-0.86	-0.59

Table 1. continued.

Name	ID	z	$\log P^T$	$\log P^C$	$\log R$	$\log R$	Name	ID	z	$\log P^T$	$\log P^C$	$\log R$	$\log R$
(1)	(2)	(3)	(4)	(5)	(6)	(7)	(1)	(2)	(3)	(4)	(5)	(6)	(7)
1305+801	Q	1.183	27.15	26.41	-0.38	-0.10	1732+160	Q	1.270	27.52	25.40	-1.84	-1.56
1308+182	Q	1.689	27.32	26.00	-1.02	-0.75	1741+279	Q	0.372	26.75	26.11	-0.25	0.03
1311-270	Q	2.195	27.80	26.66	-0.83	-0.55	1745+624	Q	3.886	28.37	28.11	0.36	0.64
1315+346	Q	1.050	26.98	26.76	0.46	0.73	1800+440	Q	0.663	26.56	26.04	-0.09	0.19
1317+520	Q	1.060	27.37	26.78	-0.18	0.09	1802+110	Q	1.132	27.37	23.63	-3.46	-3.19
1318+113	Q	2.171	28.35	26.88	-1.18	-0.90	1807+279	Q	1.760	27.66	27.29	0.15	0.42
1323+655	Q	1.618	27.44	25.71	-1.45	-1.17	1816+475	Q	2.225	27.73	26.24	-1.20	-0.92
1328+307	Q	0.849	28.18	27.88	0.28	0.55	1828+487	Q	0.692	27.94	27.30	-0.25	0.03
1330+022	Q	0.216	26.19	25.26	-0.60	-0.32	1830+285	Q	0.594	26.83	26.25	-0.17	0.11
1335+552	Q	1.096	27.11	26.96	0.66	0.94	1842+681	Q	0.475	26.54	26.29	0.39	0.66
1345+584	Q	2.039	27.61	26.41	-0.90	-0.62	1849+670	Q	0.657	26.93	26.52	0.08	0.36
1347+539	Q	0.978	27.16	26.77	0.11	0.39	1856+737	Q	0.460	26.20	26.00	0.51	0.79
1354+195	Q	0.720	27.15	26.92	0.43	0.71	1857+566	Q	1.595	27.57	25.99	-1.29	-1.02
1354+258	Q	2.032	27.32	26.44	-0.54	-0.27	1901+319	Q	0.635	27.20	26.84	0.17	0.44
1402+044	Q	3.211	28.46	28.22	0.41	0.68	1924+507	Q	1.098	27.04	26.76	0.32	0.60
1418+546	Q	1.440	28.27	27.01	-0.96	-0.68	1928+738	Q	0.302	26.58	26.49	0.91	1.19
1422+202	Q	0.871	27.29	25.56	-1.45	-1.17	1954+513	Q	1.223	27.55	27.53	1.60	1.88
1451-375	Q	0.314	26.36	26.24	0.77	1.05	2007+777	Q	0.589	26.65	25.81	-0.50	-0.22
1458+718	Q	0.904	28.01	27.62	0.11	0.39	2015+657	Q	2.845	28.17	27.83	0.20	0.48
1508-055	Q	1.180	28.32	26.88	-1.15	-0.87	2037+511	Q	1.686	28.41	28.18	0.43	0.71
1509+158	Q	0.828	26.96	26.08	-0.54	-0.27	2043+749	Q	0.104	25.30	24.71	-0.18	0.09
1510-089	Q	0.361	26.41	26.40	1.91	2.19	2120+168	Q	1.805	27.63	25.64	-1.71	-1.43
1510-089	Q	2.100	28.76	28.19	-0.16	0.12	2134+004	Q	1.932	28.50	27.37	-0.82	-0.54
1514-241	Q	1.546	26.64	25.49	-0.84	-0.57	2138+826	Q	2.350	27.95	27.51	0.03	0.31
1522+155	Q	0.628	26.36	26.24	0.77	1.05	2145+067	Q	0.990	28.19	27.84	0.18	0.46
1532+016	Q	1.440	27.78	27.07	-0.34	-0.06	2149+212	Q	1.534	27.55	26.56	-0.67	-0.39
1540+180	Q	1.662	27.93	26.91	-0.70	-0.42	2201+315	Q	0.298	26.25	26.18	1.03	1.31
1545+210	Q	0.264	26.28	24.50	-1.50	-1.22	2209+080	Q	0.484	26.52	25.83	-0.31	-0.04
1547+215	Q	1.206	27.87	23.58	-4.01	-3.74	2209+152	Q	1.502	26.85	25.98	-0.53	-0.25
1555+332	Q	0.942	26.38	23.98	-2.12	-1.85	2213-283	Q	0.946	27.00	25.83	-0.86	-0.59
1602-001	Q	1.625	27.66	27.01	-0.26	0.01	2221-023	Q	0.879	26.24	24.90	-1.04	-0.77
1606+180	Q	0.346	26.28	24.34	-1.66	-1.38	2230+114	Q	1.037	28.04	27.68	0.17	0.44
1611+343	Q	1.401	27.88	27.78	0.86	1.14	2248+192	Q	1.806	27.55	25.82	-1.45	-1.17
1618+177	Q	0.555	26.97	25.78	-0.88	-0.61	2249+185	Q	1.760	28.04	27.02	-0.70	-0.42
1622+238	Q	0.927	27.31	25.56	-1.47	-1.19	2251+134	Q	0.673	26.88	26.51	0.15	0.42
1622-297	Q	0.815	27.26	27.18	0.97	1.25	2251+158	Q	0.859	28.10	28.03	1.03	1.31
1624+416	Q	2.550	28.57	27.99	-0.17	0.11	2252+129	Q	0.555	26.79	23.76	-2.75	-2.48
1629+680	Q	2.475	28.17	27.69	-0.03	0.25	2300-189	Q	0.129	25.44	24.90	-0.12	0.16
1633+382	Q	1.814	28.19	28.01	0.57	0.84	2305+18	Q	0.313	26.08	24.78	-1.00	-0.72
1638+398	Q	1.666	27.66	27.54	0.77	1.05	2314-116	Q	0.549	25.99	25.56	0.05	0.32
1656+571	Q	1.290	27.32	26.99	0.22	0.50	2325+29	Q	1.015	27.34	26.37	-0.64	-0.37
1658+575	Q	2.173	27.79	26.48	-1.01	-0.74	2335-027	Q	1.072	27.39	26.63	-0.40	-0.12
1702+298	Q	1.927	27.93	26.41	-1.23	-0.95	2338+042	Q	2.594	27.98	27.15	-0.48	-0.21
1704+608	Q	0.371	26.65	24.14	-2.23	-1.96	2338-290	Q	0.446	26.04	25.07	-0.64	-0.37
1705+456	Q	0.648	26.84	26.25	-0.18	0.09	2349+327	Q	0.671	27.53	25.15	-2.10	-1.83
1719+357	Q	0.263	25.60	25.25	0.18	0.46	2353+283	Q	0.731	26.74	25.58	-0.85	-0.58
1721+343	Q	0.206	25.84	25.22	-0.22	0.05	2354+144	Q	1.810	27.72	26.57	-0.84	-0.57